

Control of Linear Systems with Preisach Hysteresis Output with Application to Damage Reduction

J.J. Barradas-Berglind and Rafael Wisniewski

Abstract—The focus of this work is on the Preisach hysteresis operator which has been widely used in fields such as ferromagnetics, phase transitions, filtration through porous media, and shape memory alloys. The main purpose is to incorporate discrete linear time invariant systems with discretized Preisach hysteresis output into the mixed logical dynamical (MLD) systems framework, such that the Preisach hysteresis can be included in control settings. Subsequently, an application to damage reduction is presented, where the Preisach hysteresis is used as an online fatigue damage estimator for a simplified wind turbine model. The results are evaluated for three different cases and the impact in the control effort is analyzed.

I. INTRODUCTION

Fatigue is regarded as a critical factor in structures where it is necessary to ensure a certain life span under normal operating conditions in turbulent or harsh environments. These environmental conditions lead to irregular loadings which decrease the life expectancy of structures or materials exposed to them. This is the case for wind turbines and structures in contact with waves and uneven roads, among other examples. Fatigue is a phenomenon that occurs in a microscopic scale, manifesting itself as damage. The most popular and widely used measure of fatigue damage is the so-called rainflow counting (RFC) method. Despite its widespread usage, RFC has a complex non-linear algorithmic character, which mainly limits its application as a post-processing tool. In [1], an equivalence between symmetric RFC and a type of Preisach hysteresis operator is provided, allowing to incorporate a fatigue estimator online within the control loop. However, the inclusion of hysteretic elements in the control loop is not straightforward, since hysteresis operators involve discontinuities and non-smooth nonlinearities, and in the case of the Preisach hysteresis model, infinite dimensional memory [2].

Motivation. The Preisach hysteresis operator, first introduced in [3] has been widely used in fields such as ferromagnetics, phase transitions, filtration through porous media, and shape memory alloys, and its analytical properties have been studied in works such as [2], [4], [5] and [6]. Optimal control problems with hysteresis were studied in [7] using necessary conditions for Pontryagin's extremum principle. In [8], the dynamic programming equations for controlled differential equations with hysteresis on the control input were introduced, and in [9] optimization problems for scalar systems in discrete time with Preisach hysteresis

were considered in the context of dynamic programming. In the framework of viscosity solutions of the Hamilton-Jacobi-Bellman equation, the optimal control problem was addressed for a weighted sum of delayed relays in [10] and for systems with Preisach hysteresis in [11]. Despite the theoretical soundness of the previous results, their applicability to control of complex physical systems is limited due to lack of computational tractability. In [12], the mixed logical dynamical (MLD) systems framework was introduced, which can be applied to characterize a wide variety of systems described by dynamic equations subject to linear inequalities involving real and integer variables. This is the case for linear systems with output non-linearities described by piece-wise linear functions, as shown in [12] for linear systems with saturated output.

Related work. Hybrid systems, where dynamical systems in combination with logical rules are considered, have gained a lot of attention recently and have been extensively studied [13], [14], [15], [16]. The MLD framework is intended for modeling and controlling such systems described by interdependent physical laws, logical rules, and constraints. Consequently, the inclusion of logical constraints in the control problem, as is the case of the MLD framework, results in optimization problems of a mixed integer nature, i.e., an optimization problem subject to both continuous and binary (or logical) variables [17], [18]. This allows the inclusion of discrete decision variables in the problem; e.g., whether or not to take an action. Applications of control systems in the MLD framework can be found in [19] for an active suspension system, in [20] for a DC-DC converter, and in [21] for a supermarket refrigeration system. As mentioned in [14] for systems with hysteresis, the discrete state will play a more prominent role. In [22], it was shown that the Preisach hysteresis operator can be placed in the standard dynamical system framework, since the memory is entirely contained in the state. In the present, we are interested in linear systems with Preisach hysteresis output, i.e., non-linearity in the output, which we will formulate as a collection of piece-wise linear functions to cast the system in the MLD framework.

Contribution. In this work, we cast a discrete linear time invariant system (DLTI) with discretized Preisach hysteresis output into the MLD formalism, such that these kind of systems can be directly included in control settings. In order to achieve this, we describe the discretized Preisach hysteresis as a combination of piece-wise linear functions. The contributions of this work are threefold: 1) the formulation of DLTI systems with discretized Preisach hysteresis output into the MLD formalism, 2) the direct inclusion of an online

J.J. Barradas-Berglind is with the Department of Electronic Systems, Aalborg University, Aalborg East 9220, Denmark jjb@es.aau.dk

Rafael Wisniewski is professor at the Department of Electronic Systems, Aalborg University, Aalborg East 9220, Denmark raf@es.aau.dk

fatigue estimator described by a discretized Preisach hysteresis into a receding horizon control problem under the MLD framework, and 3) the numerical studies on a simplified wind turbine model, where its practical applicability is shown, and the trade-offs inherent to the proposed strategy are evaluated.

Outline. The remainder of the paper is organized as follows: in Section II, the Preisach hysteresis operator is introduced together with its discretization procedure; in Section III, the DLTI system with discretized Preisach hysteresis output is cast into the MLD framework. An application example for damage reduction on a simplified wind turbine model is addressed in Section IV. Lastly, conclusions are presented in Section V.

A. Notation

The following notational conventions will be used in the present paper. Let \mathbb{R} and \mathbb{N} denote the set of real numbers and the set of non-negative integers, respectively. Let $\mathbb{N}_0 = \mathbb{N} \cup \{0\}$, i.e., the set of non-negative integers and zero. When the inequality signs $<$, \leq , \geq and $>$ are applied to vectors, they are interpreted element-wise. The inequality signs \prec , \preceq , \succeq , and \succ are used for matrices, e.g., for a square matrix $A \in \mathbb{R}^{n \times n}$ we write $A \prec 0$, $A \preceq 0$, $A \succeq 0$ and $A \succ 0$ when A is negative definite, negative semi-definite, positive semi-definite and positive definite, respectively. In Section III, the propositional logic connectives are used in logical statements, i.e., \wedge (and), \vee (or), \neg (not), and \rightarrow (implies).

II. PREISACH HYSTERESIS

Firstly, the notion of string and the Relay hysteresis operator are introduced, prior to addressing the Preisach hysteresis operator.

Definition 1 (Strings): Let $s = (v_0, \dots, v_N) \in S$ be a given string, which represents an arbitrary load sequence. Let S be the space of finite sequences in \mathbb{R} , i.e., $S = \{(v_0, v_1, \dots, v_N) : N \in \mathbb{N}_0, v_i \in \mathbb{R}, 0 \leq i \leq N\}$.

Definition 2 (Relay hysteresis operator): Let $\mu, \tau \in \mathbb{R}$ with $\mu < \tau$ and $w_{-1} \in \{0, 1\}$ be given. We define the relay hysteresis operator $\mathcal{R}_{\mu, \tau} : S \rightarrow S$ by

$$\mathcal{R}_{\mu, \tau}(v_0, \dots, v_N) = (w_0, \dots, w_N), \quad (1)$$

$$\text{with } w_i = \begin{cases} 1, & v_i \geq \tau, \\ 0, & v_i \leq \mu, \\ w_{i-1}, & \mu < v_i < \tau. \end{cases} \quad (2)$$

Definition 3 (Preisach hysteresis operator): Define the Preisach plane as

$$P = \{(\mu, \tau) \in \mathbb{R}^2, -M \leq \mu \leq \tau \leq M\}, \quad (3)$$

where M is an a priori bound for admissible input values. Let the density function ρ with compact support in P be given, i.e., set to zero outside the triangle P . We define the Preisach operator $\mathcal{W} : S \rightarrow S$ as

$$\mathcal{W}(s) = \int_{\mu < \tau} \rho(\mu, \tau) \mathcal{R}_{\mu, \tau}(s) d\mu d\tau. \quad (4)$$

Here, the integral is understood to be component-wise with respect to the elements of the string $\mathcal{R}_{\mu, \tau}(s)$. Consequently,

the relevant threshold values for the relays $\mathcal{R}_{\mu, \tau}$ will lie within the triangle P . The density function ρ weighting the relay operator in (4) will be further discussed in Section II-B.

A. Approximation by Discretization

The Preisach operator in (4) can be discretized or approximated by a weighted sum of relay hysterons, i.e., $\mathcal{H} = \sum_i \nu(\mu_i, \tau_i) \mathcal{R}(\mu_i, \tau_i)$, for $i \in \mathbb{N}$, as described in [5], resulting in a weighted sum of $L(L+1)/2$ relays, where L is called the discretization level. This follows the reasoning that (4) could be thought of as a weighted superposition of relays, so by discretizing we are replacing the integral by a sum, and since the integral is restricted to $\mu < \tau$ then the relays should lie inside the triangle P . The approximation is depicted in Fig. 1, where every relay has an individual weight $\nu(\mu_i, \tau_i)$.

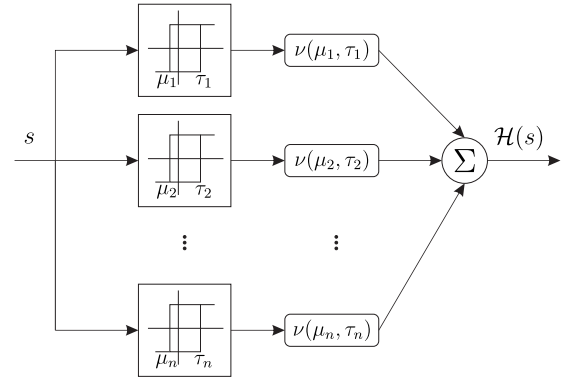


Fig. 1. The discretized Preisach operator.

Figure 2 shows the Preisach plane P for four cases of discretization level. This corresponds to uniform discretization, assuming that the density distribution inside each cell is concentrated at the center, shown as small blue circles.

B. Preisach Density Function

In order to use the Preisach operator, its density or weighting function $\rho(\mu, \tau)$ needs to be known in general; identification methods can be found in [5] and [6]. Moreover, while discretizing the Preisach operator as mentioned above, the density function $\rho(\mu, \tau)$ is captured by the weightings on each relay $\nu(\mu_i, \tau_i)$. In other words, the density function ρ might be described as a variable gain depending on the values of μ and τ .

III. CONSTRUCTION OF THE MLD SYSTEM

The intention is to cast a linear state space with discretized Preisach hysteresis output as a MLD system. Accordingly, we will have a discrete linear time invariant (DLTI) system with output Preisach hysteresis written as

$$x(k+1) = Ax(k) + Bu(k), \quad (5a)$$

$$y(k) = \mathcal{H}(\bar{z}(k), \bar{z}(k-1)), \quad (5b)$$

where $\bar{z}(k) = \bar{C}x(k)$. The system described in (5) will be cast into the MLD formalism in the sequel, first for the particular case with $L = 2$ and then generalized to $L > 2$.

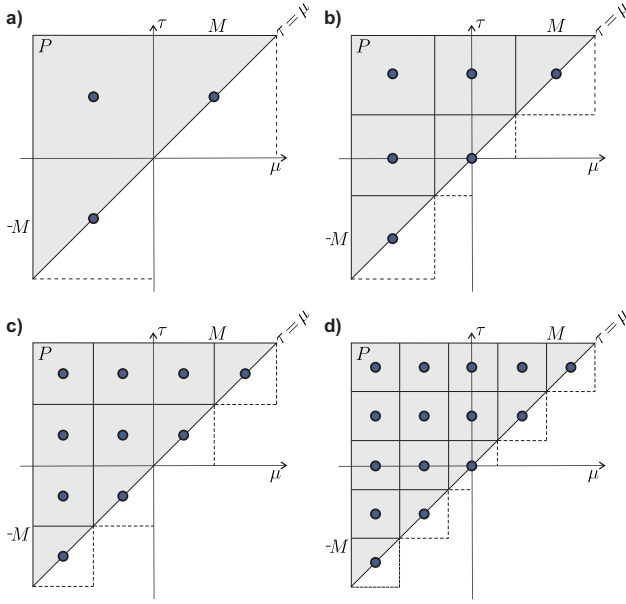


Fig. 2. Discretization of Preisach hysteresis with different levels: a) $L = 2$, b) $L = 3$, c) $L = 4$, and d) $L = 5$.

A. Discretization Level $L = 2$

In this case for illustration purposes we consider $L = 2$, but the approach is the same for an arbitrary L , which will be discussed in section III-B. Accordingly, the discretized Preisach hysteresis \mathcal{W} in (4) will be given by the sum of three relays letting the individual weight be $\nu(\mu_i, \tau_i) \equiv \nu_i$ for $i \in \{1, 2, 3\}$ such that

$$\begin{aligned} \mathcal{H}(s) &= \nu_1 \mathcal{R}_{\mu_1, \tau_1}(s) + \nu_2 \mathcal{R}_{\mu_2, \tau_2}(s) + \nu_3 \mathcal{R}_{\mu_3, \tau_3}(s) \\ &= \mathcal{H}_1(s) + \mathcal{H}_2(s) + \mathcal{H}_3(s). \end{aligned} \quad (6)$$

The intention is to represent $\mathcal{H}(s)$ as a combination of piece-wise linear (PWL) functions. From the Preisach plane as depicted in Fig. 3, assuming uniform discretization and symmetric thresholds, we can characterize each relay as

$$\mathcal{H}_1 = \nu_1 \mathcal{R}_1 = \nu_1 \mathcal{R}(\mu_1, \tau_1) = \nu_1 \mathcal{R}(-\ell, \ell), \quad (7a)$$

$$\mathcal{H}_2 = \nu_2 \mathcal{R}_2 = \nu_2 \mathcal{R}(\mu_2, \tau_2) = \nu_2 \mathcal{R}(\ell, \ell), \quad (7b)$$

$$\mathcal{H}_3 = \nu_3 \mathcal{R}_3 = \nu_3 \mathcal{R}(\mu_3, \tau_3) = \nu_3 \mathcal{R}(-\ell, -\ell), \quad (7c)$$

for some chosen value of $\ell \in P$.

From the three weighted relays in (6), \mathcal{H}_1 is a standard relay as in Definition 2, and \mathcal{H}_2 and \mathcal{H}_3 correspond to the degenerative (or memoryless) case where $\tau = \mu$. For the degenerative case, the relays can be described by the following logic rules using the boolean variables $\delta_1, \delta_2 \in \{0, 1\}$ for any relay input v , such that

$$[v \geq \ell] \rightarrow [\delta_1 = 1] \quad (\text{and } [v < \ell] \rightarrow [\delta_1 = 0]), \quad (8a)$$

$$[v \geq -\ell] \rightarrow [\delta_2 = 1] \quad (\text{and } [v < -\ell] \rightarrow [\delta_2 = 0]), \quad (8b)$$

which actually matches the same thresholds for \mathcal{H}_1 , for

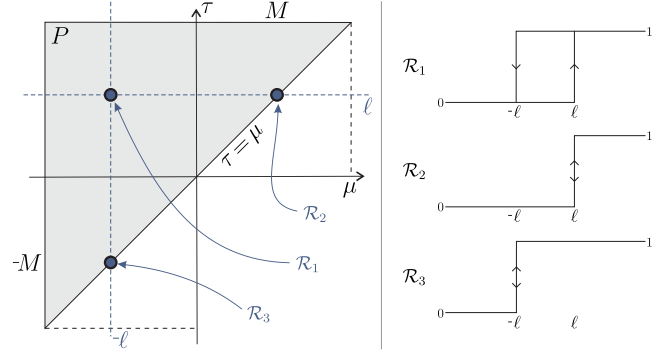


Fig. 3. Discretized Preisach operator with $L = 2$, and corresponding relays as PWL functions.

which there will be three possible regions:

$$J_1 : [v < -\ell] \rightarrow [\delta_1 = 0, \delta_2 = 0], \quad (9a)$$

$$J_2 : [-\ell \leq v < \ell] \rightarrow [\delta_1 = 0, \delta_2 = 1], \quad (9b)$$

$$J_3 : [v \geq \ell] \rightarrow [\delta_1 = 1, \delta_2 = 1]. \quad (9c)$$

The former can be reformulated to consider the bounded output $\bar{z}_{\min} \leq \bar{C}x \leq \bar{z}_{\max}$ instead of v , for some bounds \bar{z}_{\min} and \bar{z}_{\max} .

The three possible regions J_1 , J_2 , and J_3 are depicted in Fig. 3, where it can be observed that \mathcal{H}_2 can be completely characterized by δ_1 , and \mathcal{H}_3 by δ_2 . However, to characterize the standard relay \mathcal{H}_1 , we need both δ_1 , δ_2 and an additional binary state χ that remembers the previous state of the relay (w_{i-1} in (2)) for the region J_2 . Here the memory effects of the Preisach operator become evident, since we need to augment the state space with a boolean state.

The boolean state $\chi \in \{0, 1\}$ is updated (after δ_1 and δ_2 are updated) using the following condition

$$\chi(k+1) = \begin{cases} 1 & \text{if } \delta_4(k) := (\chi(k) \vee \delta_1(k)) \wedge \delta_2(k) = 1 \\ 0 & \text{otherwise.} \end{cases} \quad (10)$$

Looking at the truth table in Table I it should be easier to see that χ should be 1 for three cases: when region J_3 is active regardless e of χ , and when J_2 is active and $\chi = 1$ previously.

TABLE I
TRUTH TABLE FOR BOOLEAN STATE UPDATE

χ	δ_1	δ_2	$\chi \vee \delta_1$	$\delta_4 = (\chi \vee \delta_1) \wedge \delta_2$	Region
0	0	0	0	0	J_1
0	0	1	0	0	J_2
0	1	0	1	0	—
0	1	1	1	1	J_3
1	0	0	1	0	J_1
1	0	1	1	1	J_2
1	1	0	1	0	—
1	1	1	1	1	J_3

Subsequently, we rewrite the output of (5b) such that

$$y(k) = z_1(k) + z_2(k) + z_3(k) + z_4(k), \quad (11)$$

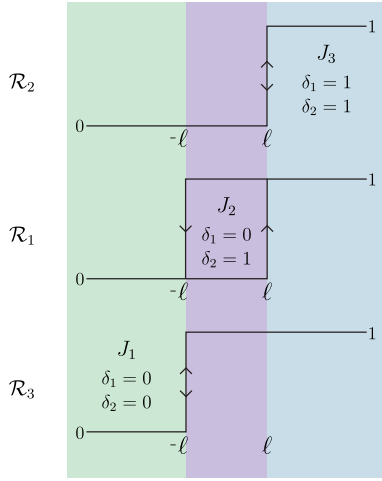


Fig. 4. Regions in the relays operation according to δ_1 and δ_2 : region J_1 in (green, left), region J_2 (violet, middle), and region J_3 (blue, right).

where $z_i \in \mathbb{R}$ for $i \in \{1, 2, 3, 4\}$ are the auxiliary continuous variables associated to the MLD form defined as

$$z_1 = \begin{cases} \nu_2 & \text{if } \delta_1(k) = 1 \\ 0 & \text{otherwise} \end{cases} \quad (12a)$$

$$z_2 = \begin{cases} \nu_3 & \text{if } \delta_2(k) = 1 \\ 0 & \text{otherwise} \end{cases} \quad (12b)$$

$$z_3 = \begin{cases} \nu_1 & \text{if } \delta_3(k) = 1 \\ 0 & \text{otherwise} \end{cases} \quad (12c)$$

$$z_4 = \begin{cases} \nu_1 & \text{if } \delta_1(k) = 1 \\ 0 & \text{otherwise,} \end{cases} \quad (12d)$$

where $\delta_3(k) := (\delta_2(k) \wedge \neg \delta_1(k)) \wedge \chi(k)$ corresponds to the contribution of \mathcal{H}_1 in region J_2 (to fully characterize the output of \mathcal{H}_1 we need both z_3 and z_4).

B. Discretization Level $L > 2$

The results presented for discretization level $L = 2$ can be generalized for the case of discretization level $L > 2$. Accordingly, the discretized Preisach operator in (5b) will be given by

$$\mathcal{H}(s) = \sum_i \nu(\mu_i, \tau_i) \mathcal{R}_{\mu_i, \tau_i}(s), \quad \text{for } i \in \mathbb{N}, \quad (13)$$

resulting in $L(L+1)/2$ relays in the Preisach plane P with coordinates (μ, τ) , of which L will lie on the line $\mu = \tau$ corresponding to the memoryless or degenerative relays. Hence, giving rise to $L(L-1)/2$ standard relays or relays with memory. Consequently, the dimension of the continuous auxiliary variables will be $\dim(z) = L + 2(L(L-1)/2) = L^2$, i.e., the number of memoryless relays plus two times the number of standard relays. The dimension of the binary auxiliary variables will be given by the sum of the number of variables needed to define regions of the relays and two times the number of standard relays (one time for the boolean state and another time for identification of the region) as

$\dim(\delta) = \dim(z) = L^2$. To exemplify the previous, the number of relays and auxiliary variables needed for the construction of the MLD system are shown in Table II, for the discretization levels depicted in Fig. 2.

TABLE II
MLD CHARACTERISTICS FOR DIFFERENT DISCRETIZATION LEVELS

Discretization level	$L = 2$	$L = 3$	$L = 4$	$L = 5$
Memoryless relays	2	3	4	5
Standard relays	1	3	6	10
Total relays	3	6	10	15
Boolean states	1	3	6	10
$\dim(z) / \dim(\delta)$	4	9	16	25

C. MLD System Description

The HYSDEL compiler [23] translates difference equations together with regular and binary constraints into a mixed logical dynamical (MLD) system of the form

$$x(k+1) = Ax(k) + B_1u(k) + B_2\delta(k) + B_3z(k), \quad (14a)$$

$$y(k) = Cx(k) + D_1u(k) + D_2\delta(k) + D_3z(k), \quad (14b)$$

$$E_2\delta(k) + E_3z(k) \leq E_1u(k) + E_4x(k) + E_5, \quad (14c)$$

where $x(k)$ is the state vector and $u(k)$ is the control inputs vector. The binary vector $\delta(k) = [\delta(k)_1, \dots, \delta(k)_{r_l}] \in \{0, 1\}^{r_l}$ of dimension r_l and the vector $z(k) \in \mathbb{R}^{r_c}$ of dimension r_c are the vectors of auxiliary variables associated with the MLD form [12].

Following the procedure described in Section III, i.e., to cast the system in (5) extended with the corresponding boolean states into the MLD formalism, the model in (14) simplifies to

$$x(k+1) = Ax(k) + B_1u(k) + B_2\delta(k), \quad (15a)$$

$$y(k) = D_3z(k), \quad (15b)$$

$$E_2\delta(k) + E_3z(k) \leq E_4x(k) + E_5, \quad (15c)$$

since B_3, C, D_1, D_2 and E_1 contain only zero elements. Note that for the case when $L = 2$ the state space in (5) is effectively extended by including the boolean state $\chi(k) = \delta_4(k)$ via the B_2 matrix in (15a).

IV. APPLICATION EXAMPLE

The goal of the application example presented here is to control a simplified wind turbine reducing the incurred fatigue in the shaft using a predictive control based strategy, see [24], [25].

A. Plant Model

For the application example we will consider a plant model given by the simplified drive-train model of a wind turbine in [26], which only considers the shaft rotational mode. The model corresponds to the linearized plant at a chosen operating point, described by the following set of differential equations

$$\dot{\varpi} = -b_1\varpi + b_2\sigma + b_3\theta - b_4\beta, \quad (16a)$$

$$\dot{\sigma} = b_5\varpi - b_6\sigma - b_7\theta - b_8\Gamma + b_9\psi, \quad (16b)$$

$$\dot{\theta} = -b_{10}\varpi + b_{11}\sigma. \quad (16c)$$

In (16), ϖ corresponds to the generator speed, σ to the rotor speed, and θ to the shaft torsion; we will consider $x = (\varpi, \sigma, \theta)$ as the vector of states. Furthermore, the inputs to the model are the collective pitch angle β , the generator torque Γ , and the variations in the wind speed ψ ; we will let $u = (\beta, \Gamma)$ be the vector of controls, and the wind we will consider as a disturbance $d = \psi$. The coefficients b_i , for $i \in \{1, 2, \dots, 11\}$ are system parameters taken from [27] after linearizing around an operating point for a mean wind speed of $18m/s$.

Lastly, we discretize the model in (16) with a chosen sampling time T_s to obtain the DLTI system

$$x(k+1) = Ax(k) + B_1u(k) + Fd(k). \quad (17)$$

B. Damage Estimation

For the damage estimation, we will lean on the equivalence provided in [1] and [2] between symmetric rainflow counting and a Preisach hysteresis operator, which is given as follows:

Proposition 1 (Damage equivalence): Let $\mathcal{W}^{per}(s)$ be the periodic version of the Preisach operator with density function $\rho(\mu, \tau)$, such that for each sequence of stresses $s = (v_0, \dots, v_N) \in S$ with $\|s\|_\infty \leq M$ and $v_0 = v_N$ the total damage $D_{ac}(s)$ associated to s satisfies

$$D_{ac}(s) = \sum_{\mu < \tau} \frac{c_{per}(s)(\mu, \tau)}{\mathcal{N}(\mu, \tau)} = \text{Var}(\mathcal{W}^{per}(s)), \quad (18)$$

where Var corresponds to the Variation operator defined as

Definition 4 (Variation): For any string $s = (v_0, \dots, v_N) \in S$, we define its variation $\text{Var} : s \rightarrow \mathbb{R}$ by

$$\text{Var}(s) = \sum_{i=0}^{N-1} |v_{i+1} - v_i|. \quad (19)$$

Following the interpretation of RFC given in [2], the left-hand side of the equivalence in (18) amounts to symmetric RFC such that $\mathcal{N}(\mu, \tau)$ denotes the number of times a repetition of the input cycle (μ, τ) leads to failure, and $c_{per}(s)(\mu, \tau)$ is the rainflow count associated with a fixed string s between the values of μ and τ . The right-hand side of (18) corresponds to the variation of the periodic Preisach operator, which is the periodic version of the Preisach operator and its density function ρ is a function of $\mathcal{N}(\mu, \tau)$. The interpretation of the previous result is that the RFC method counts the number of oscillations at each range of amplitude, and this is precisely what $\text{Var}(\mathcal{W}^{per}(s))$ calculates.

Note that the equivalence (18) uses the periodic version of (4) such that it takes into account the rainflow residual. However, in the sequel we will use the Preisach operator $\mathcal{W}(s)$ instead of its periodic version $\mathcal{W}^{per}(s)$, which amounts to consider the accumulated damage without the effect of the rainflow residual; for details on the previous refer to Theorem 2.12.6 and Corollary 2.12.7 in [2].

C. Problem Formulation

The intention is to include (18) into the problem formulation. Accordingly, we let $\bar{C} = [0 \ 0 \ 1]$ in (5b) to select

the shaft torsion θ , and from (11) we have $y = \mathcal{H}(\bar{C}x) = \mathcal{H}(\theta)$. Furthermore, as explained in [28, p.171], the total variations of a signal are equivalent to taking certain norm. Consequently, the following optimization problem is to be solved in order to control the plant model in (16) while reducing the damage in the shaft, through a term in the cost function that penalizes the variations of MLD system output y , i.e.,

$$\begin{aligned} \min_{\xi} J(\xi, x(t)) &= \sum_{k=1}^N \|Qx(k)\|_p + \sum_{k=0}^{N-1} \|Ru(k)\|_p + \sum_{k=0}^{N-1} \|Wy(k)\|_p \\ s.t. & \begin{cases} x(0) = x(t), \\ x(k+1) = Ax(k) + B_1u(k) + B_2\delta(k), \\ y(k) = D_3z(k), \\ E_2\delta(k) + E_3z(k) \leq E_4x(k) + E_5, \\ u_{\min} \leq u(k) \leq u_{\max}, \text{ for } k = 0, 1, \dots, N-1, \\ x_{\min} \leq x(k) \leq x_{\max}, \text{ for } k = 1, \dots, N, \end{cases} \end{aligned} \quad (20)$$

for some horizon $N \in \mathbb{N}$, at each time step t , where $x(t)$ is the state of the MLD system at time t , and $\xi := [u_0^\top, \dots, u_{N-1}^\top, \delta_0^\top, \dots, \delta_{N-1}^\top, z_0^\top, \dots, z_{N-1}^\top]^\top$. The weighting matrices on the states, inputs and outputs are given by $Q = Q^\top \succ 0$, $R = R^\top \succ 0$, and W as a positive scalar, respectively. Using the Hybrid Toolbox [29] the problem in (20) is translated into a mixed integer program (MIP). According to the receding horizon strategy, the first move u_0^* of the optimizer ξ^* gives the current input $u(t) = u_0^*$.

D. Simulation Results

The example was implemented in Matlab, where we considered the DLTI system with discretized Preisach hysteresis output as in (15) with the DLTI plant in (17), using a sampling time of $T_s = 0.15$ seconds. Additionally, the fatigue estimation is provided by a discretized Preisach hysteresis operator \mathcal{H} with discretization level $L = 2$, hence providing \mathcal{H} in (5b). We let $\ell = 0.05M$ such that the thresholds of the relays composing \mathcal{H} are set to $(\mu_1, \tau_1) = (-0.05M, 0.05M)$, $(\mu_2, \tau_2) = (0.05M, 0.05M)$ and $(\mu_3, \tau_3) = (-0.05M, -0.05M)$, where M is the bound for P calculated as $M = \max\{|\theta|\}$. The relay weightings were chosen as $\nu_1 = \iota$, $\nu_2 = \iota^2$, $\nu_3 = \iota^3$ for $\nu_1 + \nu_2 + \nu_3 = 1$, and their initial conditions were given according to:

$$w_{-1}(\mu, \tau) = \begin{cases} 1, & \mu + \tau < 0, \\ 0, & \mu + \tau \geq 0. \end{cases} \quad (21)$$

The HYSDEL compiler [23] was used to translate the difference equations and constraints into the MLD formalism as in (15). The controller synthesis was carried out using the Hybrid Toolbox [29] letting $p = \infty$ in (20), such that the cost functional $J(\xi, x(t))$ amounts to the sum of a weighted mixed 1- and ∞ -norm of the inputs, state and output deviations, namely the 1-norm with respect to time of the ∞ -norm with respect to space. The simulation was carried out for 500 seconds and the horizon was set to $N = 2$.

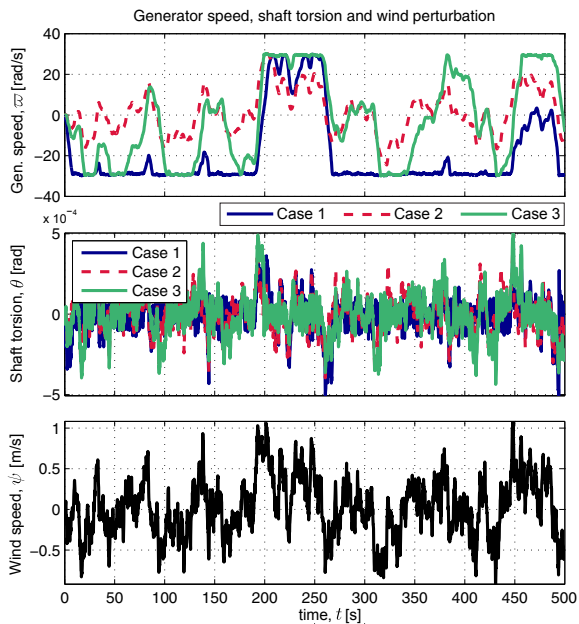


Fig. 5. Generator speed, shaft torsion and wind speed perturbation.

The weighting matrices for the cost functional in (20) were selected as follows for three different cases:

- *Case 1 - Damage reduction:* Q and R are diagonal with elements $(0, 0, q_3, 0)$ and (r_1, r_2) , and $W = 10$.
- *Case 2 - Bryson's rule:* Q and R are diagonal with elements $(q_1, q_2, q_3, 0)$ and (r_1, r_2) , and $W = 0$.
- *Case 3 - Intermediate:* Q and R are diagonal with elements $(0, 0, q_3, 0)$ and (r_1, r_2) , and $W = 1$.

where the elements of Q and R were chosen according to Bryson's rule [30, p.537] such that $(q_1, q_2, q_3, q_4) = (1/30^2, 1/0.3^2, 1/0.001^2, 0)$ and $(r_1, r_2) = (1/30^2, 1/0.1^2)$, respectively, and the boolean state is unpenalized. The limits on inputs and states were considered as $u_{\max} = [30, 0.001]$, $u_{\min} = [-30, -0.001]$, $x_{\max} = [30, 0.3, 0.001, 1]$, and $x_{\min} = [-30, -0.3, -0.001, 0]$. We set initial conditions to $x(0) = (0, 0, 0, 0)$, and ψ was taken from wind series data.

It is worth noting that the MLD formalism does not handle disturbances directly; in order to include the wind perturbation ψ in (16) in the simulation two models were used, namely one for controller synthesis with two inputs, and one for simulation with three inputs where we additionally inject ψ as an exogenous input. Alternatively, this inclusion may be achieved by embedding a model of the disturbance, or by means of an observer. A good choice would be to estimate the wind speed via the rotor torque, as proposed in [26]; however, this would result in an increased number of states.

The simulation results are shown in Fig. 5-7, for the three cases defined above. Fig. 5 shows the generator speed ϖ , the shaft torsion θ , and the wind speed ψ ; the rotor speed σ is omitted, since its behavior is quite similar to ϖ . The collective pitch angle β and the generator torque Γ are shown in Fig. 6, from which we can observe that the collective pitch exhibits more fluctuations and the torque is almost constant, which corresponds to operating region of

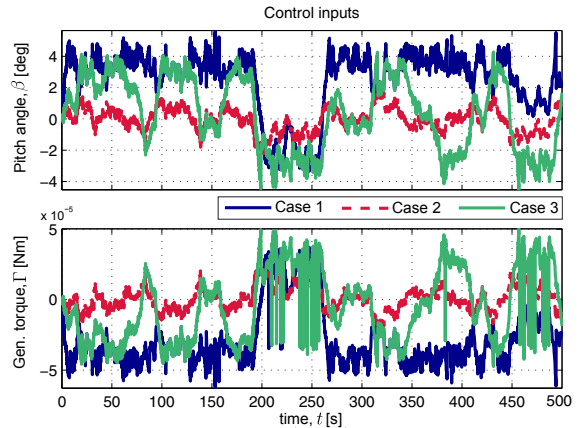


Fig. 6. Control inputs: pitch angle and generator torque.

the chosen operating point. Lastly, in Fig. 7 the output of the MLD system $y = \mathcal{H}(\theta)$, and the accumulated damage in the shaft $\text{Var}(\mathcal{H}(\theta))$ are presented, where it can be observed that the damage reduction scheme corresponding to Case 1 successfully reduced the damage, because the control strategy discourages the switches in the output.

Nevertheless, if one carefully observes Fig. 6, Case 1 seems to exert more pitch activity in comparison to Cases 2 and 3, which would result in increased wear in the pitch actuator. Thus, to shed some light on the matter, we calculated for each case the accumulated damage on the pitch angle derivative, i.e., $\mathcal{H}(\dot{\beta})$ as post-processing, where we low-passed $\dot{\beta}$, considered $L = 2$, set the relay weightings to $\bar{v}_1 = \bar{v}_2 = \bar{v}_3 = 1/3$, and adjusted the thresholds of the relays according to $\bar{\ell} = 0.15\bar{M}$ with $\bar{M} = \max\{|\dot{\beta}|\}$; the results are shown in Fig. 8. From Fig. 7 and 8, we can conclude that there is a trade-off between the damage in the shaft and the pitch activity, namely, Case 1 achieves damage reduction in the shaft increasing the pitch activity, while Case 2 leads to more damage in the shaft, but less pitch activity. Lastly, Case 3 corresponds to an intermediate scenario.

The data, parameters and scripts used in this example are available online at <https://kom.aau.dk/~jjb/>.

V. CONCLUSIONS

In this paper, we cast DLT systems with discretized Preisach hysteresis output into the MLD formalism, which allows these kind of systems to be directly incorporated in optimal control problem formulations. Accordingly, the HYSDEL compiler can be used to generate the MLD system and then it can be interfaced with toolboxes such as the Hybrid Toolbox or the MPT toolbox [31] using MATLAB.

Furthermore, we present an application example for fatigue damage reduction, where the discretized Preisach operator is used as an online damage estimator. In this example, we propose a solution that successfully reduces the damage in the shaft of a simplified wind turbine plant model, showing the practical applicability of this approach. However, there exists a trade-off between the damage in the component and the control effort, which we also illustrated.

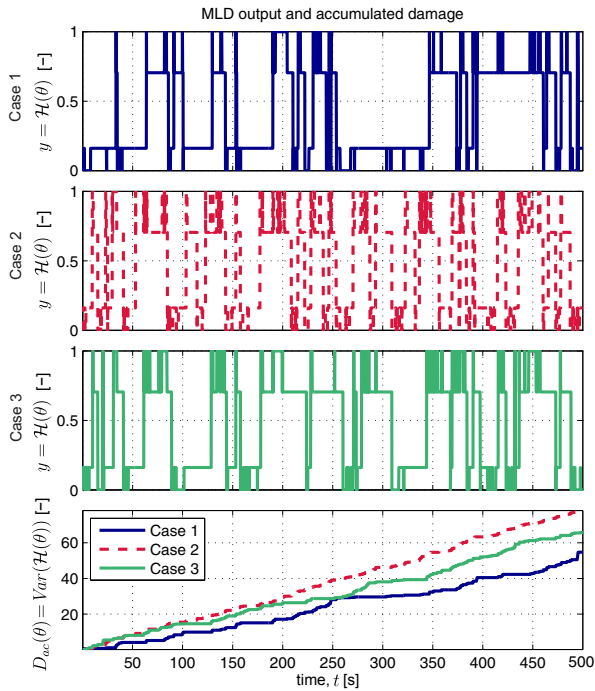


Fig. 7. MLD system output and accumulated damage on the shaft for Cases 1, 2 and 3.

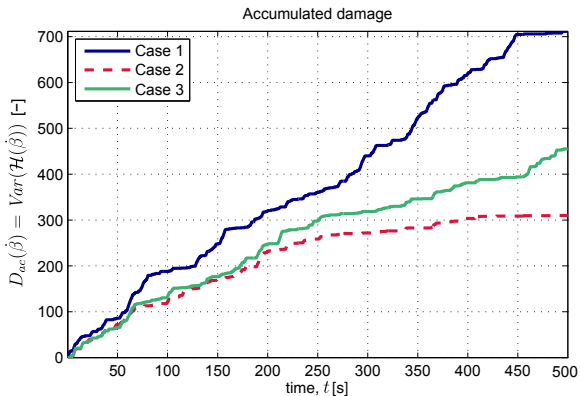


Fig. 8. Accumulated damage on $\hat{\beta}$ for Cases 1, 2 and 3.

VI. ACKNOWLEDGMENTS

This work was partially supported by the Danish Council for Strategic Research (contract no. 11-116843) within the ‘Programme Sustainable Energy and Environment’, under the ‘EDGE’ (Efficient Distribution of Green Energy) research project.

REFERENCES

- [1] M. Brokate, K. Dreßler, and P. Krejčí, “Rainflow counting and energy dissipation for hysteresis models in elastoplasticity,” *European J. of Mech. A/Solids*, vol. 15, no. 4, pp. 705–737, 1996.
- [2] M. Brokate and J. Sprekels, *Hysteresis and phase transitions, volume 121 of Applied Mathematical Sciences*. Springer-Verlag, 1996.
- [3] F. Preisach, “Über die Magnetische Nachwirkung,” *Zeitschrift für Physik*, vol. 94, no. 5-6, pp. 277–302, 1935.
- [4] M. A. Krasnosel’skiĭ and A. V. Pokrovskiĭ, *Systems with hysteresis*. Springer Verlag, 1989.
- [5] I. D. Mayergoyz, *Mathematical Models of Hysteresis*. Springer-Verlag, 1991.

- [6] A. Visintin, *Differential models of hysteresis*. Springer Berlin, 1994.
- [7] M. Brokate, *Optimale Steuerung von Gewöhnlichen Differentialgleichungen mit Nichtlinearitäten vom Hysteresis-Typ*. P. Lang, 1987, vol. 35.
- [8] S. Belbas and I. Mayergoyz, “Dynamic programming for systems with hysteresis,” *Physica B: Condensed Matter*, vol. 306, no. 1, pp. 200–205, 2001.
- [9] S. Belbas and I. Mayergoyz, “Optimal control of dynamical systems with Preisach hysteresis,” *Int. J. of Non-linear Mech.*, vol. 37, no. 8, pp. 1351–1361, 2002.
- [10] F. Bagagiolo, “An infinite horizon optimal control problem for some switching systems,” in *Discrete and Continuous Dynamical Sys., Series B*. Citeseer, 2001.
- [11] F. Bagagiolo, “Viscosity solutions for an optimal control problem with Preisach hysteresis nonlinearities,” *ESAIM: Control, Optimisation and Calculus of Variations*, vol. 10, no. 02, pp. 271–294, 2004.
- [12] A. Bemporad and M. Morari, “Control of systems integrating logic, dynamics, and constraints,” *Automatica*, vol. 35, no. 3, pp. 407–427, 1999.
- [13] M. S. Branicky, “Multiple Lyapunov functions and other analysis tools for switched and hybrid systems,” *IEEE Trans. Aut. Control*, vol. 43, no. 4, pp. 475–482, 1998.
- [14] M. Johansson and A. Rantzer, “Computation of piecewise quadratic Lyapunov functions for hybrid systems,” *IEEE Trans. Aut. Control*, vol. 43, no. 4, pp. 555–559, 1998.
- [15] W. Heemels, B. De Schutter, and A. Bemporad, “Equivalence of hybrid dynamical models,” *Automatica*, vol. 37, no. 7, pp. 1085–1091, 2001.
- [16] C. J. Tomlin, J. Lygeros, and S. S. Sastry, “A game theoretic approach to controller design for hybrid systems,” *Proc. of the IEEE*, vol. 88, no. 7, pp. 949–970, 2000.
- [17] G. L. Nemhauser and L. A. Wolsey, *Integer and combinatorial optimization*. Wiley New York, 1988, vol. 18.
- [18] R. Raman and I. E. Grossmann, “Modelling and computational techniques for logic based integer programming,” *Computers & Chemical Eng.*, vol. 18, no. 7, pp. 563–578, 1994.
- [19] N. Giorgetti, A. Bemporad, H. E. Tseng, and D. Hrovat, “Hybrid model predictive control application towards optimal semi-active suspension,” *Int. J. of Control*, vol. 79, no. 05, pp. 521–533, 2006.
- [20] T. Geyer, G. Papafotiou, and M. Morari, “Hybrid model predictive control of the step-down dc–dc converter,” *IEEE Trans. Control Sys. Tech.*, vol. 16, no. 6, pp. 1112–1124, 2008.
- [21] L. F. Larsen, T. Geyer, and M. Morari, “Hybrid model predictive control in supermarket refrigeration systems,” in *Proc. of the IFAC World Congress*, 2005.
- [22] R. Gorbet, K. Morris, and D. Wang, “Control of hysteretic systems: a state-space approach,” in *Learning, control and hybrid systems*. Springer, 1999, pp. 432–451.
- [23] F. D. Torrisi and A. Bemporad, “HYSDEL—a tool for generating computational hybrid models for analysis and synthesis problems,” *Control Systems Technology, IEEE Transactions on*, vol. 12, no. 2, pp. 235–249, 2004.
- [24] M. Soltani, R. Wisniewski, P. Brath, and S. Boyd, “Load reduction of wind turbines using receding horizon control,” in *IEEE Int. Conf. on Control Applications (CCA)*. IEEE, 2011, pp. 852–857.
- [25] J. Barradas-Berglind, R. Wisniewski, and M. Soltani, “Fatigue damage estimation and data-based control for wind turbines,” *IET Control Theory & Applications*, 2015.
- [26] K. Z. Østergaard, P. Brath, and J. Stoustrup, “Estimation of effective wind speed,” in *J. of Physics: Conf. Series*, vol. 75, no. 1. IOP Publishing, 2007, p. 012082.
- [27] J. M. Jonkman, S. Butterfield, W. Musial, and G. Scott, *Definition of a 5-MW reference wind turbine for offshore system development*. NREL, 2009.
- [28] H. Logemann and E. P. Ryan, “Systems with hysteresis in the feedback loop: existence, regularity and asymptotic behaviour of solutions,” *ESAIM: Control, Opt. and Calc. of Var.*, vol. 9, pp. 169–196, 2003.
- [29] A. Bemporad, “Hybrid Toolbox-user’s guide,” 2003.
- [30] G. Franklin, J. Powell, and A. Emami-Naeini, *Feedback control of dynamic systems*. Addison-Wesley Reading, 1994, vol. 3.
- [31] M. Kvasnica, P. Grieder, M. Baotić, and M. Morari, “Multi-parametric toolbox (MPT),” in *Hybrid systems: computation and control*. Springer, 2004, pp. 448–462.